CrossMark

A Revised Earthquake Catalogue for South Iceland

Francesco Panzera,[1,2] J. Douglas Zechar,[3] Kristín S. Vogfjörd,[1] and David A. J. Eberhard[3]

Abstract—In 1991, a new seismic monitoring network named SIL was started in Iceland with a digital seismic system and automatic operation. The system is equipped with software that reports the automatic location and magnitude of earthquakes, usually within 1–2 min of their occurrence. Normally, automatic locations are manually checked and re-estimated with corrected phase picks, but locations are subject to random errors and systematic biases. In this article, we consider the quality of the catalogue and produce a revised catalogue for South Iceland, the area with the highest seismic risk in Iceland. We explore the effects of filtering events using some common recommendations based on network geometry and station spacing and, as an alternative, filtering based on a multivariate analysis that identifies outliers in the hypocentre error distribution. We identify and remove quarry blasts, and we re-estimate the magnitude of many events. This revised catalogue which we consider to be filtered, cleaned, and corrected should be valuable for building future seismicity models and for assessing seismic hazard and risk. We present a comparative seismicity analysis using the original and revised catalogues: we report characteristics of South Iceland seismicity in terms of *b value* and magnitude of completeness. Our work demonstrates the importance of carefully checking an earthquake catalogue before proceeding with seismicity analysis.

1. Introduction

In a recent report from the London Workshop on the Future of Statistical Sciences (Madigan *et al.* 2014), the responsibilities of a statistician were defined as:

- to design the acquisition of data in a way that minimizes bias and confounding factors and maximizes information content;

- to verify the quality of the data after those are collected; and

- to analyse data in a way that produces insight or information to support decision-making

As statistical seismologists, our work tends to emphasize the third point, with little thought given to the others: we often treat earthquake catalogues as collections of perfect measurements, forgetting (or at least neglecting) that a hypocentre location is the uncertain result of an unsolved inversion problem; and we are almost never involved in planning data collection or seismic network design. With this article, we address the second responsibility, which directly supports the third responsibility, future data analyses. In particular, we consider the quality of the data in the earthquake catalogue generated by the SIL seismic network in Iceland.

The SIL network was planned and developed in the framework of the Nordic SIL project in 1988–1994 (Stefánsson *et al.* 1993; Böðvarsson *et al.* 1996, 1999). The network was originally installed and operated in South Iceland in 1990 to monitor seismicity in the South Iceland Seismic Zone (SISZ), a sinistral transform zone that crosses southern Iceland. In 1993, it was expanded to the seismic zone in northern Iceland, thereby becoming a national network for Iceland, covering the country's two main seismic zones. In the following years, the network was gradually expanded along the rift zones that cross Iceland from southwest to northeast (pink colour in Fig. 1a). In 1994, SIL included 18 stations and by the end of 2013 the seismic network had grown to 68 stations (Fig. 1a).

South Iceland is a rather densely populated farming area with many small towns and several critical infrastructures, such as hydropower plants and associated reservoirs, geothermal power plants,

[1] Icelandic Meteorological Office, Reykjavík, Iceland. E-mail: panzerafrancesco@hotmail.it
[2] Università di Catania, Dipartimento di Scienze Biologiche, Geologiche e Ambientali, Catania, Italy.
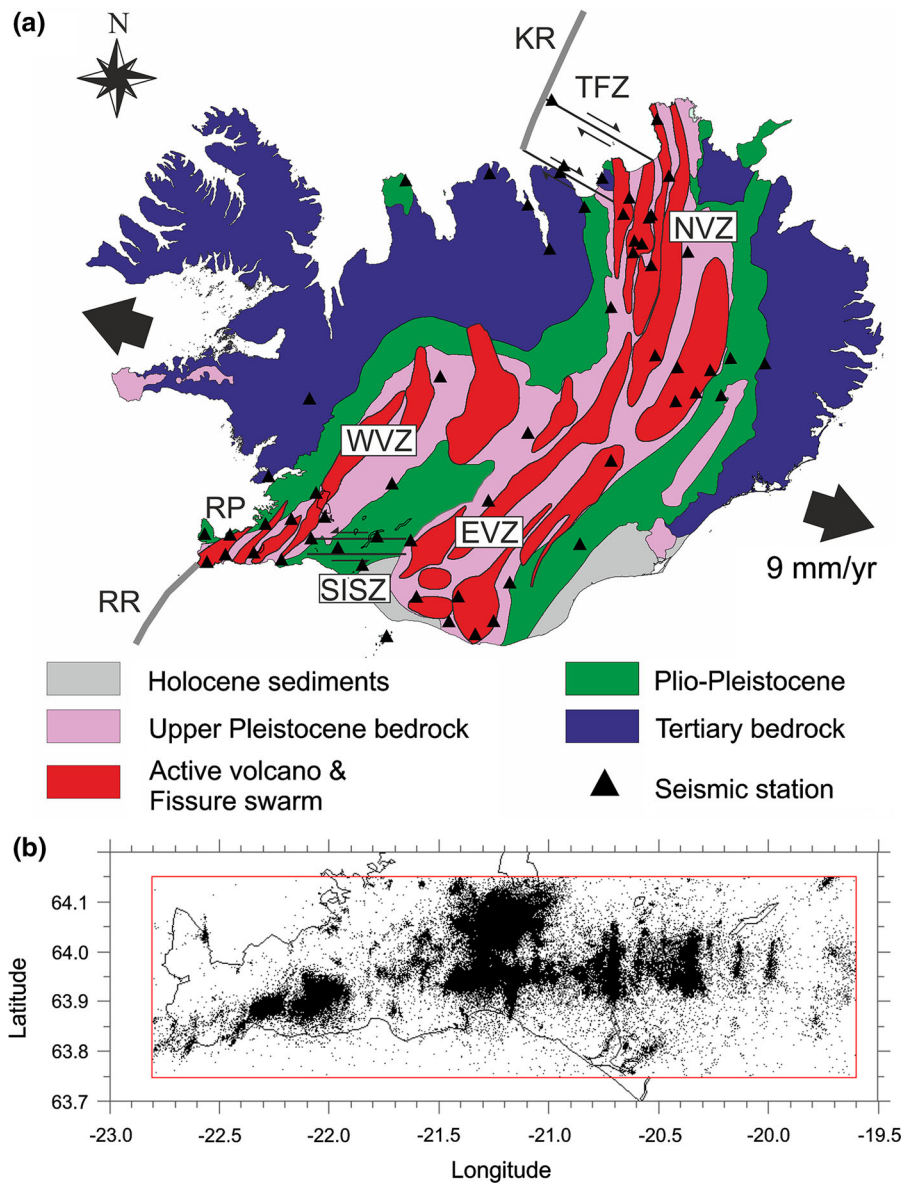[3] Swiss Seismological Service (SED), ETH, Zurich, Switzerland.

Figure 1

a Schematic representation of the plate boundary in Iceland (modified from ANGELIER *et al.* 2004). **b** Map of the study area. *Black dots* events in the selected catalogue. *EVZ* Eastern Volcanic Zone, *NVZ* Northern Volcanic Zone, *KR* Kolbeinsey Ridge, *RP* Reykjanes Peninsula, *RR* Reykjanes Ridge, *TFZ* Tjörnes Fracture Zone, *SISZ* South Iceland Seismic Zone, *WVZ* Western Volcanic Zone

industrial plants and transportation infrastructures. More hydropower plants and reservoirs are planned in the area in coming years. Because of the presence of human population and critical infrastructures, southern Iceland has the highest seismic risk in the country. We would like to build models to mitigate the seismic risk; almost any such model one can imagine requires a seismicity catalogue as input and,

therefore, we study the SIL catalogue to obtain a first-order understanding of seismicity in this region and to understand the quality of the catalogue. Moreover, since the year 2000 a major earthquake sequence is ongoing in the study area, where three earthquakes of $M_W > 6$ have already occurred and more events of up to moment magnitude (M_W) 7.0 can be expected in the coming years to decades (EINARSSON *et al.* 1981;

DECRIEM *et al.* 2010). The historical seismicity in this region is well known (EINARSSON *et al.* 1981; AMBRASEYS and SIGBJÖRNSSON 2000) and many major faults have been mapped on the surface (EINARSSON *et al.* 1981; BERGERAT and ANGELIER 2000; CLIFTON and EINARSSON 2005) and at depth by high-precision locations (HJALTADÓTTIR *et al.* 2005; HJALTADÓTTIR 2009).

Quality check of the seismic catalogue is important because results obtained from a contaminated dataset may be misleading (GULIA *et al.* 2012). To make such a check, careful identification of man-made changes should represent the first step in any statistical analysis of seismicity. Such changes, for example, redefining the magnitude scale in a catalogue may introduce errors in statistical analyses of seismicity patterns and they mislead researchers by generating spurious apparent variations in the observed seismicity rate (HABERMANN 1987; TORMANN *et al.* 2010). Our catalogue check emphasizes removing events with very high or even unknown location uncertainty (filtering), removing quarry blasts (cleaning), and re-estimating magnitudes (correcting). After this filtering and corrections to the reported magnitudes, we report a spatio-temporal analysis of South Iceland seismicity based on *b* value and magnitude of completeness. The revised SIL catalogue is available from us upon request, and it should be used as the starting point for future analyses and modelling of South Iceland seismicity.

2. Tectonic Setting

In this section, we give only a brief summary of the regional tectonics (for more details, see EINARSSON 1991).

The complex tectonic setting of Iceland is linked to the eastward shifting of the Mid-Atlantic Ridge axis, a consequence of its westward migration away from the hotspot currently situated under the Vatnajökull glacier (EINARSSON 2008). As illustrated in Fig. 1a, this movement gives rise in southern Iceland to two sub-parallel volcanic zones. The first is the continuation of the Atlantic Ridge that comes on shore on the Reykjanes Peninsula (RP) and continues as the Western Volcanic Zone (WVZ). The second,

the Eastern Volcanic Zone (EVZ), which continues in northern Iceland as the Northern Volcanic Zone (NVZ), is shifted eastward along the SISZ transform zone. Finally, in northern Iceland the rift shifts back westward along the Tjörnes Fracture Zone (TFZ) to connect with the Kolbeinsey Ridge (KR).

The SISZ is a 10–20-km-wide, EW striking sinistral shear zone, but faulting occurs on sub-parallel, NS striking dextral faults (HACKMAN *et al.* 1990; ROTH 2004), as demonstrated by the shape of the damage zones of historical earthquakes (EINARSSON *et al.* 1981; AMBRASEYS and SIGBJÖRNSSON 2000), their mapped surface traces (EINARSSON 1991; CLIFTON and EINARSSON 2005) and subsurface fault mapping by high-precision earthquake relocations (HJALTADÓTTIR 2009).

The RP is a highly oblique spreading segment of the Mid-Atlantic Ridge, oriented about 30° from the direction of absolute plate motion (CLIFTON and KATTENHORN 2006). There are four distinct volcanic fissure swarms on the peninsula (JAKOBSSON *et al.* 1978), with an average strike of 40°N. Similar to the SISZ, large earthquakes on Reykjanes peninsula occur on NS striking faults that intersect the volcanic fissure swarms (ÁRNADÓTTIR *et al.* 2004; KEIDING *et al.* 2008; CLIFTON *et al* 2003; ANTONIOLI *et al.* 2006).

3. Data Collection and Magnitude Estimation

The initial earthquake catalogue considered for this study spans the period 1991–2013 and contains 205,016 earthquakes with depth ranging between 0 and 50 km and with $M_L \geq -2.0$. The selected area includes both the SISZ and the RP and is within the limits 63.75° to 64.15° in latitude and −22.8° to −19.6° in longitude (Fig. 1b). Originally, the incoming seismic data were pre-processed by a computer at the site of each seismic station and transients were detected and defined by onset time, amplitude, and duration. Apparent velocity, azimuth, and spectral parameters were calculated, and this information was packed into short messages and sent to the data centre at the Icelandic Meteorological Office in Reykjavík, where an automatic phase association process defined events and sent requests

for waveform data to the stations (Böðvarsson *et al.* 1996). In 2013–2014, transmission of continuous waveforms was initiated for all the sites and the analysis was moved to the data centre at IMO. Automatic locations and magnitudes of earthquakes are usually available within 1–2 min of their occurrence. These are manually reviewed by analysts at the SIL data centre. This includes readjusting or adding phase arrivals where necessary, relocating events and recalculating magnitudes. This process is a routine operation and special evaluation of larger events is not part of the analysis.

The SIL system uses two methods to estimate each earthquake's magnitude. The first is based on an empirical local magnitude relationship:

$$M_L = \log_{10}(A) + 2.1 \log_{10}(D) + 4.8 \qquad (1)$$

where A is the maximum velocity amplitude in m/s of high-pass filtered waveforms with a corner frequency (f) at 1.5 Hz and scaled to the response of Lennartz 1.0 Hz sensor and Nanometrics RD3 digitizer, and D is the epicentral distance in km (Gudmundsson *et al.* 2006).

The other magnitude scale is a "local" moment magnitude scale, M_{LW} that was originally constructed by Slunga *et al.* (1984) to agree with local magnitude scales in Sweden:

$$M_{LW} = \log_{10}(m_0) - 10, \quad \text{for } M_{LW} \leq 2.0 \quad (2)$$

where m_0 is the seismic moment in Nm (Rögn-valdsson and Slunga 1993). For magnitudes above 2.0, the formula is slightly modified so that the slope decreases with increasing magnitude (Pétursson and Vogfjörd 2009). In particular, considering the factor:

$$m = \log_{10}(m_0) - 10 \qquad (3)$$

the M_{LW} formula becomes:

$$M_{LW} = m \quad \text{for } m \leq 2.00 \qquad (4a)$$

$$M_{LW} = 2.0 + (m - 2.00) \cdot 0.9 \quad \text{for } 2.00 < m \leq 3.11 \qquad (4b)$$

$$M_{LW} = 3.0 + (m - 0.89) \cdot 0.8 \quad \text{for } 3.11 < m \leq 5.11 \qquad (4c)$$

$$M_{LW} = 4.6 + (m + 1.1) \cdot 0.7 \quad \text{for } 5.11 < m \leq 6.25 \qquad (4d)$$

$$M_{LW} = 5.4 + (m + 2.25) \cdot 0.5 \quad \text{for } 6.25 < m \leq 7.25 \qquad (4e)$$

$$M_{LW} = 5.9 + (m + 3.25) \cdot 0.4 \quad \text{for } 7.25 < m \leq 9.25 \qquad (4f)$$

$$M_{LW} = 6.3 + (m + 5.25) \cdot 0.35 \quad \text{for } 9.25 < m \quad (4g)$$

4. Verifying the Quality of the Data and Revising the Catalogue

In this section, we consider the quality of the SIL catalogue and revise it in three stages: we remove events with very large or unknown location uncertainty (filtering); we identify and delete quarry blasts that were misidentified as earthquakes (cleaning); and we re-estimate magnitudes (correcting). The procedure is illustrated in Fig. 2, including the number of events affected at each stage, and the three stages are described in the following three subsections.
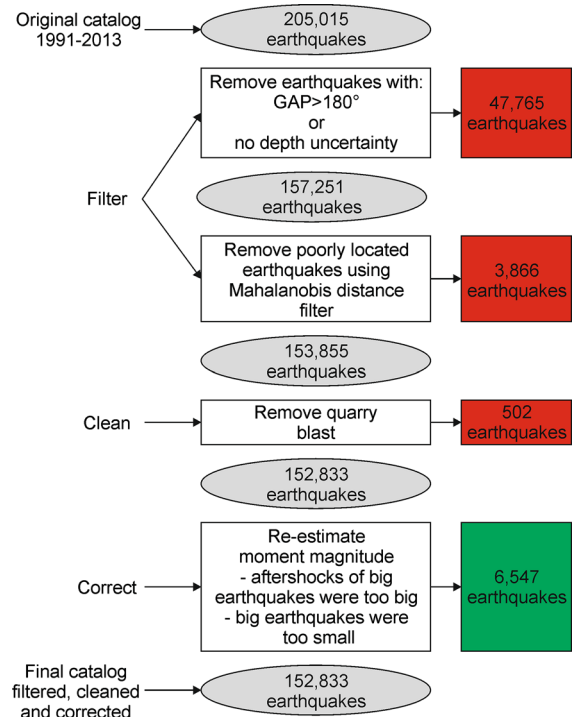

Figure 2
Flowchart that summarizes the filtering, cleaning, and correcting used to produce the revised catalogue. *Boxes in the right column* the number of events affected by each step

4.1. Earthquake Location Precision: Filtering the Catalogue

Despite all the checks in the SIL system, often earthquakes stored in the catalogue are not well located, have large azimuthal GAP (the largest angle between any two stations that recorded the earthquake), and large uncertainties in latitude, longitude, and depth (blue histograms in Fig. 3). Workers have suggested many methods to filter a catalogue so that those events that are not well located are removed. The most popular of these are the network criteria methods (NCM) discussed by GOMBERG et al. (1990), BONDAR et al. (2004), and HUSEN and HARDEBECK (2010). These authors proposed to keep only the events with GAP smaller than 180° and with at least 8 arrival times for P and S waves, of which at least one is an S wave arrival time. We applied this filter to the SIL catalogue (red histograms in Fig. 3), but the SIL network is less dense than regional networks elsewhere and, therefore, these criteria seem to be too restrictive, especially for microseismicity.

Uncertainties in earthquake locations arise from (unknown) errors in seismic arrival times, network geometry, signal-to-noise ratio, dominant frequency of the arriving phase, and the velocity model used for the location, so any catalogue should include uncertainty estimates for each earthquake's latitude, longitude, and depth. We used these estimates directly as an alternative to filter the catalogue. As in the NCM, we removed all the earthquakes with GAP higher than 180°. Noting that a histogram of the depth distribution (Fig. 4; left panel) shows spikes at exact depths 0, 1, 3, and 5 km, we also removed all earthquakes without any estimate of depth error, i.e. $D_E = 0$. These represent earthquake locations for which the location program did not converge to a solution, and thus the SIL analyst fixed the depth at 0, 1.3, or 5 km.
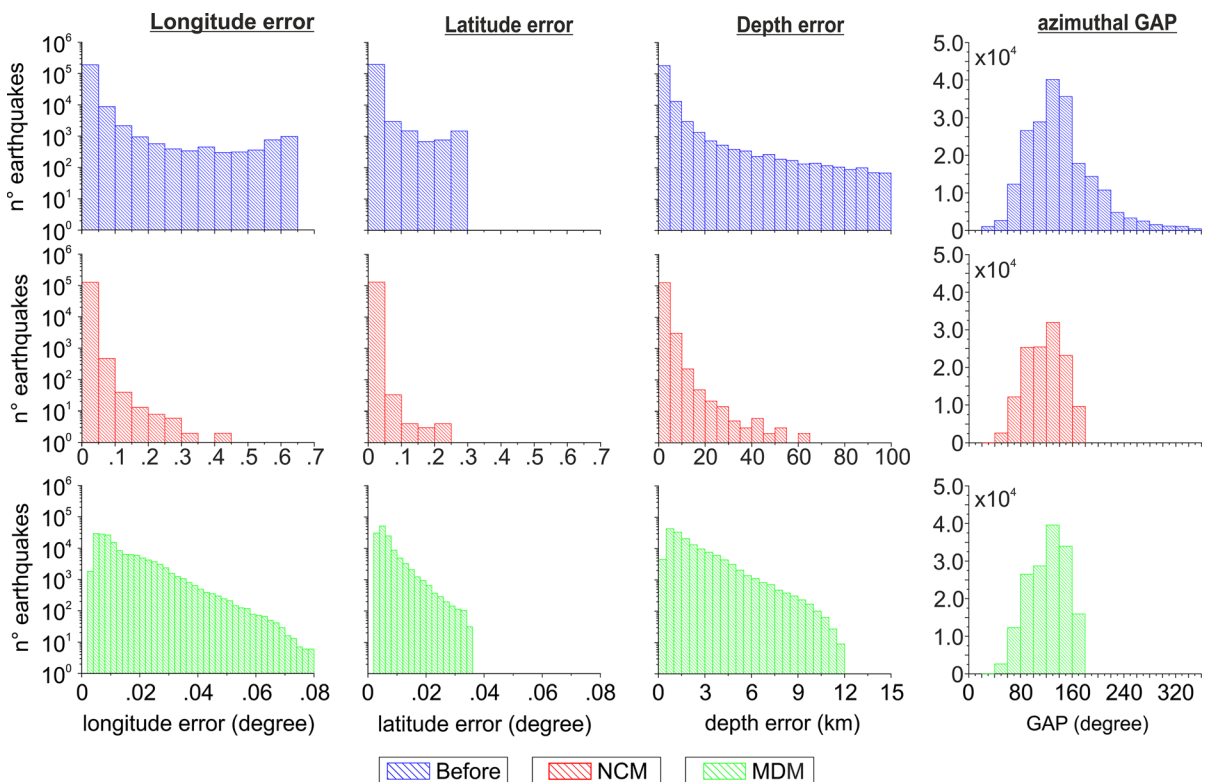

Figure 3
Histograms showing the distribution of longitude, latitude, and depth errors as well as azimuthal gap before (*blue*) and after the filtering by the network criteria method (NCM, *red*) and the Mahalanobis distance method (MDM, *green*). Note that for the *first 3 columns* the scale is semi-logarithmic, and in the *third row* a different scale for error histograms is used
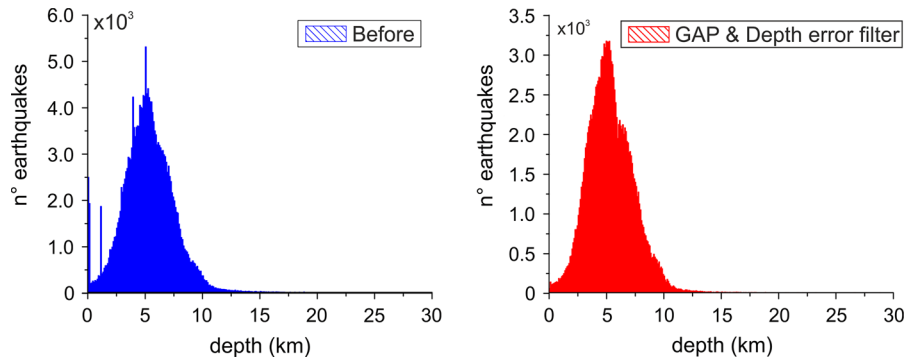
Figure 4
Distribution in depth before filtering (*blue*) and after removing GAP > 180° and $D_E = 0$ (*red*)

After removing these events with large GAP and artificially fixed depths, we applied a technique commonly used in multivariate analysis to identify outliers: filtering based on Mahalanobis distance (e.g. EVERITT 2005, Section 1.4). We treat the uncertainties in latitude, longitude, and depth as multivariate data and compute the Mahalanobis distance for each earthquake; this is the distance of a point $x(x_1; x_2; x_3)$ from the population mean $\mu(\mu_1; \mu_2; \mu_3)$:

$$d_m(\vec{x}) = \sqrt{(\vec{x} - \vec{\mu})^T S^{-1} (\vec{x} - \vec{\mu})} \qquad (5)$$

where S^{-1} is the inverse covariance matrix of the independent variables. Then, if the data distribution is multivariate normal, the squared Mahalanobis distances should follow a Chi-squared (χ^2) distribution with p degrees of freedom satisfying:

$$(\vec{x} - \vec{\mu})^T S^{-1} (\vec{x} - \vec{\mu}) \leq \chi_p^2(\alpha) \qquad (6)$$

where p is the dimension of the data (in our case, 3) and α is the probability of an equal or larger value. We take $\alpha = 0.05$, and the corresponding χ^2 critical value is 7.82. Consequently any earthquake that has a squared Mahalanobis distances in the tail of the corresponding χ^2 distribution (i.e. with value higher than 7.82) is considered an outlier and removed. We call this the MDM (Mahalanobis Distance Method).

The NCM did reduce the mean error in the catalogue (Table 1), but many earthquakes with large uncertainties in latitude, longitude and depth remained (see the second row of Fig. 3 and note the different scale for the second and third rows). On the other hand, the MDM results in a catalogue of earthquakes with a much narrower distribution of location uncertainties. Moreover, the MDM-filtered catalogue contains 153,385 earthquakes compared to the 118,823 using NCM. Because it contains more, and more precise, information, we proceed with the MDM-filtered catalogue. The MDM method is appropriate for an area like South Iceland, where the network is optimized to record microearthquakes. These events are well located despite not being recorded by several seismic stations (e.g. 4–5 seismic stations). The MDM filter could be applied also in areas that are not optimized for microearthquakes detection because it filters based on the uncertainties directly, whereas the NCM filter uses network criteria as a proxy.

4.2. Analysis of Explosion Contamination–Cleaning the Catalogue

For analysis of seismicity, the SIL catalogue should only contain earthquakes, but sometimes quarry blasts are erroneously identified as earthquakes. These explosion events have low magnitudes and produce an enrichment in the number of small earthquakes; such an increase of microseismicity may be misinterpreted as a change in the natural phenomena (GULIA *et al.* 2012).

A histogram of the number of seismic events during each hour of the day is one way to identify the presence of blasts. In a contaminated catalogue, the plot is characterized by a peak during daytime hours (WIEMER and BAER 2000). As noted by GULIA *et al.* (2012), this behaviour is due to the fact that during

Table 1

Range of GAP, and mean and standard deviation of the latitude, longitude, and depth errors during the filtering process

	Before filtering	After removing GAP > 180° and $D_E = 0$	NCM	MDM
GAP (degree)	37°–360°	37°–179.9°		37°–179.9°	37°–179.9°
Longitude (degree)	0.027° ± 0.070°	0.014° ± 0.024°	0.009 ± 0.008	0.012° ± 0.006°
Latitude(degree)	0.013° ± 0.031°	0.007° ± 0.011°	0.005° ± 0.003°	0.005° ± 0.004°
Depth (km)	2.956 ± 6.680	2.247 ± 3.509	1.506 ± 1.404	1.904 ± 1.531
Eq. number	205,015	157,251	118,823	153,385

daytime ambient noise interferes with the detection of earthquakes and a decrease in the number of detected events is generally observed, whereas the quarry-rich areas show the opposite trend. The SIL catalogue, after filtering by Mahalanobis distance, seems to be only slightly contaminated by the presence of explosions. A small peak observed in the activity around noon is likely due to less human noise during lunch hour, when stations are not affected by traffic and industrial activity (Fig. 5a). Moreover, contamination by explosions is found when areas around the cities are analysed in more detail.

To identify blasts, in Fig. 5b we present a map of the ratio of the number of daytime events to the number of nighttime events using the WIEMER and BAER (2000) algorithm. This normalized ratio, Rq, is defined as:

$$Rq = \frac{NdLn}{NnLd} \quad (7)$$

where Nd is the total number of events in the daytime, Nn in the nighttime, Ld is the number of hours in the daytime period and Ln in the nighttime period. The ratio is calculated using a regularly spaced grid covering the studied area. We used a spatial grid of 0.03° in latitude and 0.07° in longitude that gives approximately equal distance in km, and sampled the 100 nearest events to each node. The quarry contamination map is then obtained using the nearest neighbour gridding method. It is important to highlight that interpolation algorithms may show edge effects, especially when the data are not homogenously distributed. To reduce edge effects, we only identify anomalous behaviour where earthquakes have occurred (see Fig. 1b for earthquakes location).

In the obtained map, as suggested by GULIA et al. (2012), areas with $Rq \geq 1.5$ are identified as areas contaminated by explosions. In particular, using interactively selected polygons all the areas with Rq higher than 1.5 were selected and removed. The resulting map shows that the study area is only contaminated by explosions along the Reykjanes peninsula coast, at Helguvík, Hafjarfjördur, east Reykjavík, and in the south near Thorlákshöfn. This result is also supported by the hourly distribution of events for such areas (Fig. 5b).

This analysis led to removal of 502 events that were recognized as explosions, resulting in a catalogue of 152,883 earthquakes.

4.3. *Problems with Magnitudes: Correcting the Catalogue*

In the left panel of Fig. 6 are the M_L versus M_{LW} magnitude values from the filtered and cleaned catalogue. Many events fall above the 1:1 line, indicating that M_{LW} gives magnitude values higher than those obtained using M_L. The difference between the two magnitude scales seem to increase for larger earthquakes. This behaviour is probably due to the fact that M_L is a better estimate for small earthquakes, but for large earthquakes it underestimates the magnitude because short-period seismometers and high-pass filtering ($f > 1.5$ Hz) are used. We also note that the theoretical M_{LW} values derived from SLUNGA et al. (1984) for the magnitude range $1.8 < M_{LW} < 6.6$, are larger than global M_W, while outside this range M_{LW} is smaller (Fig. 6; right panel).

In addition to these systematic discrepancies—i.e. the M_L underestimation of large events and the non-linear behaviour of the M_{LW} scale—there are other problems in the SIL magnitude estimates. In particular the two main concerns are: (1) the underestimation of the m_0 of large earthquakes in the routine processing performed to obtain M_{LW} in the SIL catalogue (RÖGNVALDSSON and SLUNGA 1993)
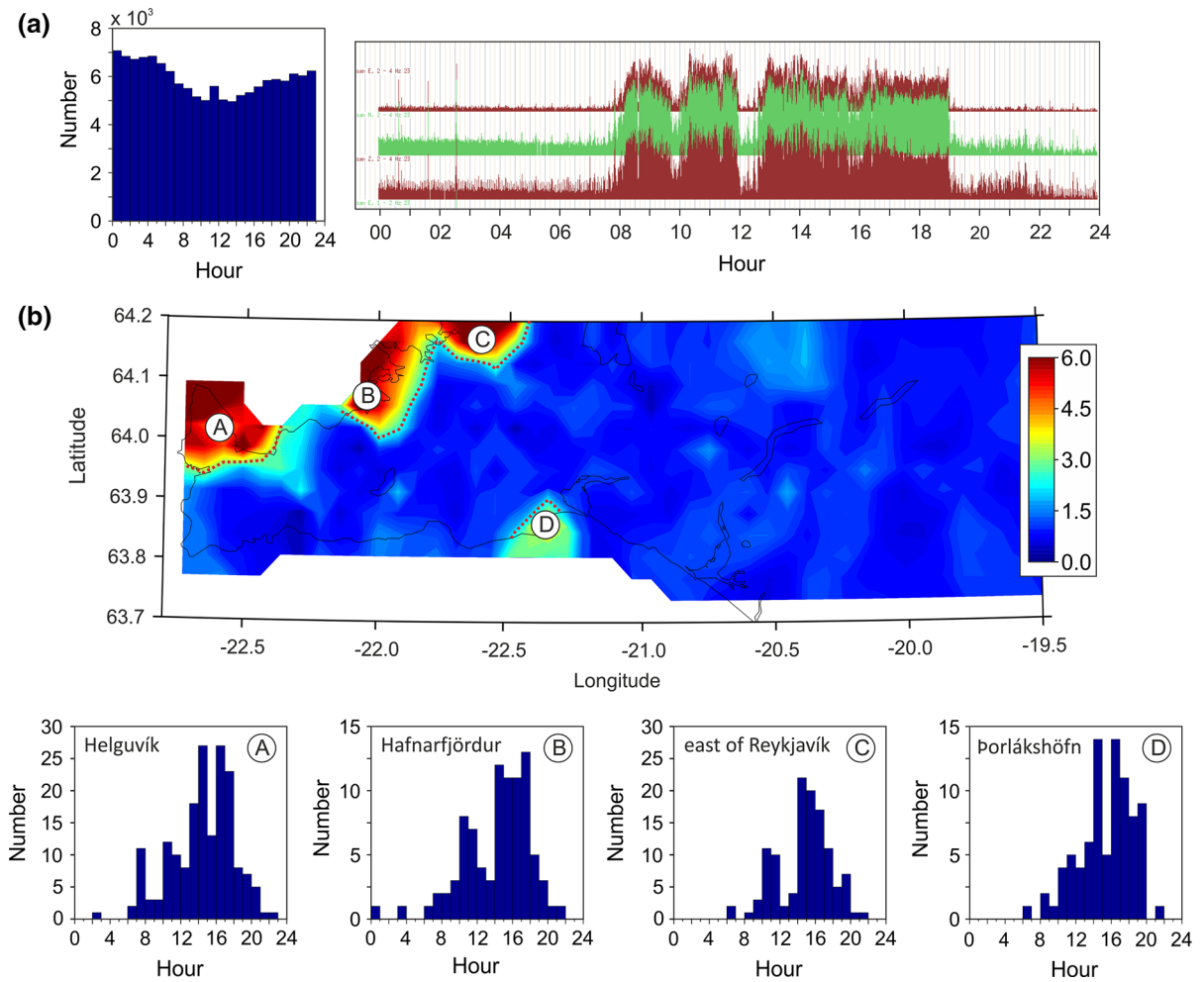
Figure 5

a *Histogram* of the number of events per hour of the day for the catalogue after the application of the Mahalanobis distance filter and example of noise amplitude versus time at the station *san*, which is located near a quarry. **b** Map of the ratio between daily and nightly events and histograms of the number of events per hour of the day for suspected areas

Figure 6

Left panel M_L versus M_{LW} scatter plot in which the *red line* is a line with slope one and *yellow ellipse* contains outliers due to erroneous magnitude estimates. *Right panel* the comparison between the M_{LW} and M_W magnitudes

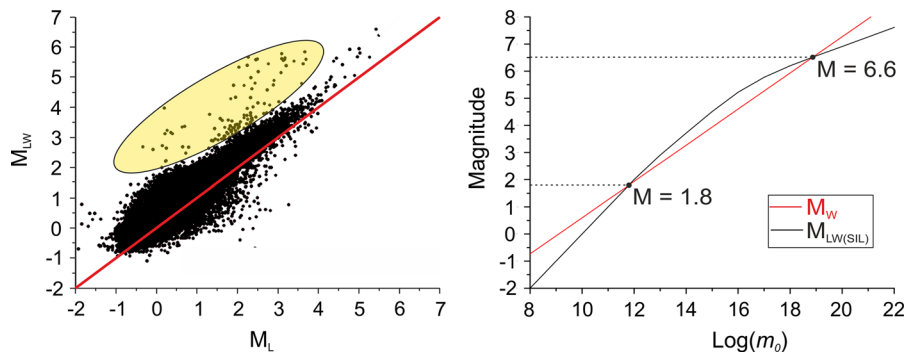and (2) the overestimation of magnitude assigned to aftershocks of big earthquakes, due to contamination by the mainshocks.

The main reason for the underestimated m_0 is that for large earthquakes, the routine analysis window around the P and S waves is too short to contain all of the source time function, and the frequency band within which the corner frequency of the source spectrum is searched does not extend to low enough frequencies. Additionally, most of the SIL seismic stations have short-period seismometers (0.2 and 1 Hz) that do not extend to sufficiently low frequencies to allow for undisturbed calculation of seismic moment for the largest earthquakes. The underestimation of m_0 becomes evident for M_{LW} greater than 3.0, which corresponds to an M_L of about 2.5.

Table 2 shows that the moment magnitude of larger earthquakes obtained using m_0 in the SIL catalogue ($M_{W\text{-}SIL}$) is severely underestimated compared to the magnitudes ($M_{W\text{-}GCMT}$) reported in the Global Centroid Moment Tensor catalogue (GCMT; DZIEWONSKI et al. 1981; EKSTRÖM et al. 2012). Consequently it is not possible to use the seismic moment (m_0), which is used for estimating M_{LW}, to directly estimate M_W. Another evidence of the problem concerning m_0 estimation is shown in the left panel of Fig. 6 (yellow ellipse), where we highlight outliers characterized by surprisingly large values of M_{LW} given their M_L. These are erroneous M_{LW} values assigned to aftershocks of big earthquakes, and the errors are caused by contamination of the waveform from the mainshock. Usually, the overestimation of aftershock magnitudes occurs in the first few minutes after the mainshock. We suspect that the low-frequency component of the mainshock coda waves make the corner frequency appear to be lower than it should be.

For all these reasons the magnitude values in the catalogue must be corrected before any statistical analysis. Although the M_L estimate is influenced by the high-pass filtering, we prefer to use these estimates to find a method for magnitude correction, because they are more stable than the M_{LW} estimates. Moreover, there are 902 earthquakes in the catalogue with M_L higher than 2.5 for which it is necessary to make the correction, and it would be very time-consuming to re-compute the seismic moment for all of these earthquakes.

To correct magnitudes, we used a technique based on peak ground velocity magnitude (M_{PGV}) estimates using an attenuation relationship for South Iceland (PÉTURSSON and VOGFJÖRD 2009). This relationship uses an empirical form for the decay of peak ground velocity and acceleration (PGV and PGA) with distance based on waveforms from 45 events in southern Iceland in the magnitude range $3.0 \leq M_W \leq 6.5$ and for distances in the range 5–300 km. The relations were scaled with M_W and include a non-linear, near-source term. A log-linear approximation to the relation, valid outside the near-source region, is a robust real-time measure of magnitude for events of $M_w \geq 3.0$. The log-linear part of the equation for velocity is:

$$\log_{10}(\text{PGV}) = -1.63 \log_{10}(r) + M - 4.88 \quad (8)$$

where r is the epicentral distance in km and M is the moment magnitude. For our study we used Eq. (8) to estimate M_{PGV} through the reverse formula:

Table 2

List of earthquakes in South Iceland for which the GCMT reports a moment magnitude. In the table $M_{W\text{-}SIL}$ are the underestimated moment magnitude values obtained by using the seismic moment in the SIL catalogue, named $m_0(SIL)$, whereas $M_{W\text{-}GCMT}$ and $m_0(GCMT)$ are corresponding values in Global Centroid Moment Tensor catalogue

Dd/mm/yy	Origin time	$M_{W\text{-}SIL}$	$M_{W\text{-}GCMT}$	$M_0(SIL)$ (dyne·cm)	$M_0(GCMT)$ (dyne·cm)
04/06/98	21:36:53.81	4.4	5.4	4.96×10^{22}	1.56×10^{24}
13/11/98	10:38:34.42	4.5	5.1	5.93×10^{22}	5.43×10^{23}
17/06/00	15:40:40.98	6.2	6.5	2.36×10^{23}	7.05×10^{25}
21/06/00	00:51:46.99	6.6	6.4	1.03×10^{26}	5.44×10^{25}
23/08/03	02:00:11.79	4.4	5.1	4.90×10^{22}	5.96×10^{23}
29/05/08	15:45:58.91	5.1	6.3	6.16×10^{23}	3.38×10^{25}
29/05/08	21:33:49.11	4.3	4.8	3.70×10^{22}	2.21×10^{23}

$$M_{PGV} = \log_{10}(PGV) + 1.63 \log_{10}(r) + 4.88 \quad (9)$$

This equation is also used in the Icelandic real-time ShakeMap system (VOGFJÖRD et al. 2012; Icelandic Meteorological Office website: http://hraun.vedur.is/ja/alert/shake/). This type of approach was used with good results by several authors in others part of the world (e.g. LIN and WU 2010; ESHAGHI et al. 2013).

To calibrate a conversion between M_L with M_{PGV}, we used the 45 events used by PÉTURSSON and VOGFJÖRD (2009) and additional 59 events taken from the Icelandic ShakeMap website (all events are listed in Table 3).

We fit a generalized orthogonal regression (GOR) model to the data in Table 3 to describe the relationship between M_{PGV} and M_L (Fig. 7, left panel). We used GOR rather than standard least-squares because the two magnitude scales have similar uncertainties (CASTELLARO et al. 2006). The resulting GOR relationship is:

$$M_{PGV} = (1.215 \pm 0.031) M_L + (-0.373 \pm 0.110), \\ M_L \geq 2.5$$

$$(10)$$

We used Eq. (10) to correct estimates of $M_{PGV} \approx M_W$ for all the earthquakes with M_L higher than 2.5, since those are events for which the seismic moment is thought to be underestimated with respect to the GCMT catalogue. For earthquakes with M_L lower than 2.5 we used the SIL seismic moment to estimate M_W. After these corrections, we performed comparisons among the derived M_{PGV}, M_{W-SIL}, M_{W-GCMT} and body wave magnitude (m_b) from the International Seismological Centre (ISC) catalogue (STORCHAK et al. 2013). In Fig. 8a (left panel) we present M_{PGV} versus M_{W-GCMT} for 14 earthquakes in South Iceland (Table 4) reported in the GCMT catalogue. We noted that the relationship is nearly 1:1 between M_{PGV} and M_{W-GCMT}. Since 14 events are too few and the M_W magnitude range is short, for a better comparison we used also m_b for 38 events from the ISC catalogue with magnitudes in the range 3.5–6.0 (Table 4). We fitted a GOR model using M_{PGV} and m_b (Fig. 8a, right panel) and then we compared the obtained model with that proposed by WASON et al. (2012). Although the number of events

used and the range of magnitudes considered by WASON et al. (2012) are different from those of our analysis, there seems to be a good agreement between the two models (Fig. 8a, right panel). On the contrary, as already discussed concerning the problems with the SIL magnitude estimates, Fig. 8b highlights a poor correlation among the M_{W-SIL}, M_{W-GCMT} and m_b listed in Table 4.

This procedure allowed us to overcome the problem of underestimated seismic moment for events with $M_L \geq 2.5$. However, below M_L 2.5 there are several earthquakes with poorly estimated local moment magnitude (yellow ellipse in the left panel of Fig. 6), and we also seek to correct these. To correct the erroneous moment magnitudes of earthquakes with $M_L < 2.5$, we divided the earthquakes by M_L into bins of ± 0.1 (see Table 5) and for each bin we calculated the mean value and two standard deviations (2σ) of M_W (see Table 5), obtained from the SIL seismic moment. For each bin any earthquake having an M_W more than 2σ from the mean were considered outliers. For these outliers, we used a linear relationship between the M_L central values and M_W mean values in Table 5 to estimate a corrected M_W:

$$M_W = 0.7654 + 0.6944 M_L, \quad \sigma = 0.0326, \\ 0.0 \leq M_L < 2.5$$

$$(11)$$

Following this procedure, we corrected the moment magnitude estimates of 5645 earthquakes.

After these magnitude re-estimations, we have a revised catalogue that has been filtered, cleaned, and corrected. Again, we refer you to Fig. 2 for a graphical summary. In the next section, we describe an analysis of the revised catalogue, which contains 152,833 earthquakes.

5. Analysis of Seismicity

5.1. Magnitude of Completeness and b value

Estimating the magnitude of completeness, M_C, is important for analysing earthquake rate changes, mapping seismicity parameters, forecasting seismicity, and assessing seismic hazard. It is defined as the magnitude above which all events in a given space

Table 3

List of M_L and M_{PGV} used to obtain the conversion law in Eq. ([10]). M_{PGV} of 45 events was taken from PÉTURSSON and VOGFJÖRD ([2009]), while the additional 59 events are computed using Eq. ([8])

Dd/mm/yyyy	Hh:mm:ss	Lat	Lon	Depth	M_L	M_{PGV}
20/11/1992	10:28:33	63.93	−21.98	6.8	3.8	4.3
27/12/1992	12:23:22	64.02	−21.18	0.8	4.2	4.6
19/09/1993	10:00:31	63.89	−22.26	5.3	3.0	3.6
17/08/1994	06:29:30	64.06	−21.19	3.0	3.6	4.0
19/08/1994	19:18:42	64.03	−21.25	1.5	3.9	4.3
20/08/1994	16:40:26	64.04	−21.24	1.7	3.9	4.4
30/04/1995	00:57:59	64.07	−21.16	3.4	3.7	4.2
23/07/1995	09:28:55	64.06	−21.32	5.2	3.4	3.6
20/08/1995	16:57:04	64.07	−21.22	2.1	3.1	3.9
27/12/1995	04:26:07	64.07	−21.39	0.0	3.1	3.7
14/03/1996	05:34:57	64.04	−21.21	4.1	3.6	4.0
14/10/1996	20:59:58	64.05	−21.05	4.2	3.8	4.4
23/02/1997	00:35:48	63.93	−22.08	4.6	3.6	4.0
23/02/1997	08:45:03	63.94	−22.08	4.3	3.6	4.1
12/04/1997	23:04:44	64.07	−21.24	3.7	3.8	4.3
24/08/1997	03:20:02	64.05	−21.26	4.6	3.7	4.0
24/08/1997	03:04:22	64.03	−21.26	5.4	4.4	5.0
29/12/1997	10:37:31	64.02	−21.18	5.2	3.4	3.8
03/06/1998	06:47:42	64.06	−21.26	4.1	3.6	4.0
03/06/1998	18:46:09	64.07	−21.21	3.5	3.0	3.6
03/06/1998	23:23:49	64.07	−21.17	4.3	3.4	3.9
04/06/1998	12:23:27	64.04	−21.31	4.2	3.5	3.9
04/06/1998	19:04:45	64.07	−21.30	4.0	4.0	4.6
04/06/1998	21:36:54	64.04	−21.29	5.9	4.7	5.5
04/06/1998	22:04:40	64.05	−21.29	4.8	3.3	3.9
04/06/1998	22:59:57	63.99	−21.31	3.1	4.0	4.8
13/11/1998	10:38:34	63.96	−21.35	5.0	4.6	5.2
13/11/1998	10:46:31	63.96	−21.38	9.5	4.1	4.3
14/11/1998	04:36:40	63.94	−21.41	5.3	3.6	4.2
14/11/1998	04:21:14	63.94	−21.39	4.2	4.0	4.2
14/11/1998	14:24:07	63.96	−21.24	4.4	4.4	5.0
30/11/1998	10:41:16	63.93	−22.00	5.6	3.6	4.1
25/05/1999	13:19:40	64.06	−21.15	5.3	4.0	4.3
25/05/1999	18:03:05	64.05	−21.18	5.6	3.2	3.5
20/07/1999	06:04:02	63.90	−22.03	5.4	2.7	3.1
27/09/1999	16:01:15	63.97	−20.79	6.0	4.2	4.5
28/09/1999	21:50:20	63.98	−20.79	4.9	3.8	4.1
18/04/2000	19:49:08	64.06	−21.32	3.9	3.0	3.4
17/06/2000	15:40:41	63.97	−20.37	6.4	5.5	6.4
17/06/2000	15:42:51	63.94	−20.46	6.0	5.0	5.7
17/06/2000	16:24:04	64.06	−21.31	4.1	3.6	4.1
21/06/2000	00:51:47	63.97	−20.71	5.0	5.4	6.5
23/08/2003	02:00:12	63.91	−22.09	3.7	4.3	5.0
07/01/2004	23:25:25	64.02	−21.22	6.2	3.7	4.0
06/03/2006	14:31:55	63.92	−21.92	8.1	4.2	4.5
20/11/2007	18:48:54	63.95	−20.99	1.8	3.1	3.5
29/05/2008	15:46:06	63.97	−21.06	5.1	5.3	6.3
03/06/2008	19:49:00	63.92	−21.18	4.2	3.1	3.4
04/11/2008	17:47:27	63.86	−22.44	5.0	3.6	3.8
06/12/2008	14:16:34	63.97	−21.42	7.2	3.4	3.9
29/04/2009	02:57:56	63.95	−21.26	7.8	3.8	3.9
08/05/2009	19:27:11	63.94	−21.41	7.6	2.7	3.2
29/05/2009	21:33:50	63.89	−22.34	6.4	4.2	4.7
30/05/2009	02:00:04	63.88	−22.33	5.3	3.0	3.5

Table 3 *continued*

Dd/mm/yyyy	Hh:mm:ss	Lat	Lon	Depth	M_L	M_{PGV}
30/05/2009	02:05:07	64.02	−22.36	6.2	2.8	3.0
30/05/2009	07:47:43	63.92	−22.27	7.7	2.8	3.0
30/05/2009	08:33:08	63.92	−22.27	6.1	2.9	3.2
30/05/2009	13:35:23	63.91	−22.27	6.6	4.0	4.3
30/05/2009	15:13:14	63.94	−22.25	6.7	2.8	3.0
30/05/2009	16:11:16	63.91	−22.32	5.4	2.8	3.1
30/05/2009	17:05:39	63.91	−22.25	7.5	3.7	3.9
31/05/2009	07:45:14	63.90	−22.32	7.4	2.8	3.0
19/06/2009	18:13:20	63.88	−22.09	4.5	3.9	4.2
19/06/2009	20:37:13	63.89	−22.09	4.9	3.8	4.1
25/06/2009	17:20:17	63.91	−22.01	5.6	3.7	4.0
25/06/2009	19:20:33	63.92	−21.99	6.5	3.1	3.3
31/07/2009	23:46:22	63.92	−22.07	5.0	2.7	3.0
19/08/2009	13:42:16	63.91	−21.99	6.2	3.0	3.2
08/02/2010	22:08:25	63.86	−22.76	10.9	2.8	3.0
10/02/2010	16:48:06	63.72	−22.98	9.5	2.8	3.0
21/05/2010	18:56:56	64.07	−20.55	6.1	3.0	3.0
31/05/2010	07:33:25	63.95	−21.39	7.4	3.0	3.1
13/12/2010	12:58:09	63.89	−22.04	5.0	2.7	3.1
25/12/2010	17:03:54	63.93	−22.03	5.6	3.0	3.1
27/02/2011	05:20:33	63.94	−22.04	4.4	2.7	3.1
27/02/2011	05:46:03	63.92	−22.03	4.1	3.0	3.3
27/02/2011	09:05:59	63.92	−22.02	4.9	3.6	4.0
27/02/2011	09:11:13	63.90	−22.04	4.7	2.8	3.1
27/02/2011	09:16:11	63.89	−22.02	4.4	2.8	3.1
27/02/2011	09:48:42	63.93	−22.04	4.6	3.0	3.0
27/02/2011	17:27:36	63.91	−22.03	4.7	3.8	4.2
02/03/2011	08:32:18	63.93	−22.05	4.4	2.8	3.1
02/03/2011	17:56:53	63.89	−22.04	4.1	3.5	3.5
12/08/2011	04:03:17	63.93	−21.98	9.6	3.1	3.0
16/08/2011	22:14:18	63.85	−22.44	2.4	3.3	3.6
17/08/2011	01:34:23	63.85	−22.38	5.4	3.1	3.1
23/09/2011	15:10:16	64.06	−21.38	5.1	2.6	3.1
23/09/2011	15:20:04	64.06	−21.39	4.9	2.8	3.3
23/09/2011	15:22:46	64.05	−21.38	3.9	3.0	3.4
07/10/2011	11:00:31	64.05	−21.41	4.1	2.7	3.0
08/10/2011	23:04:14	64.06	−21.40	2.8	3.1	3.3
15/10/2011	09:00:46	64.07	−21.41	2.4	2.8	3.1
15/10/2011	09:03:08	64.05	−21.42	3.3	3.7	4.0
15/10/2011	09:46:04	64.07	−21.40	2.0	3.9	4.0
27/11/2011	10:17:06	63.91	−22.14	5.8	2.6	3.0
03/01/2012	21:12:42	63.89	−22.09	4.8	3.8	4.0
01/03/2012	00:29:16	64.00	−21.82	4.2	3.2	3.6
01/03/2012	01:03:07	63.99	−21.81	4.3	4.0	4.2
21/04/2012	22:36:40	64.05	−21.43	4.0	2.7	3.2
30/08/2012	11:59:02	64.00	−21.59	5.5	3.9	4.6
01/09/2012	16:33:47	63.89	−22.25	7.3	2.8	3.0
13/10/2013	09:38:52	63.83	−22.64	5.8	3.3	3.1
07/01/2014	12:11:49	64.00	−21.84	0.2	3.2	3.1

and time are expected to be detected by a seismic network (WOESSNER and WIEMER 2005; SCHORLEMMER and WOESSNER 2008; MIGNAN and WOESSNER 2012).

Most methods for assessing the magnitude of completeness rely on the Gutenberg–Richter (GR; GUTENBERG and RICHTER 1944) relation that describes the frequency of earthquake magnitudes:
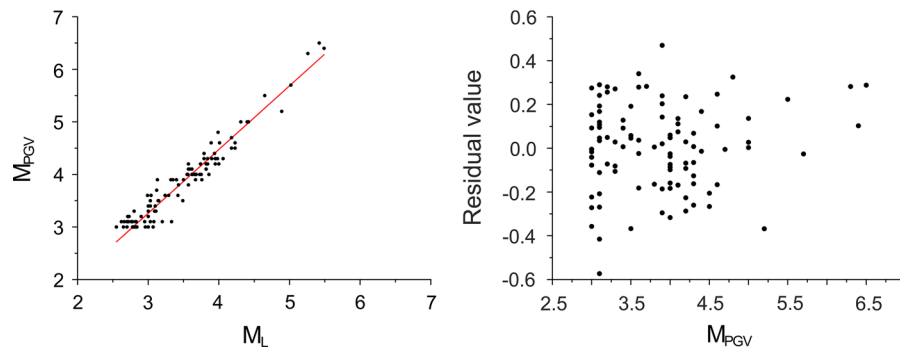
$$\log_{10} N(\geq M) = a - bM, \tag{12}$$

Figure 7
Left panel M_L versus M_{PGV}, *red line* the best fit obtained using generalized orthogonal regression. *Right panel* residual values of predicted M_{PGV} using Eq. (10) for the earthquakes listed in Table 2
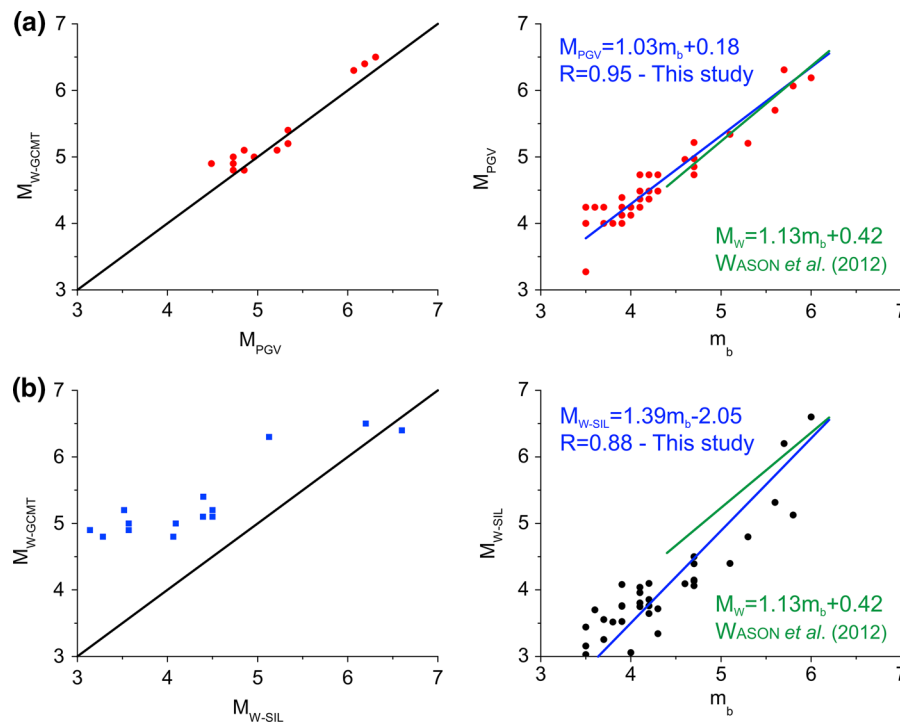

Figure 8
Comparisons of the derived M_{PGV}, M_{W-SIL}, M_{W-GCMT} and m_b for the earthquakes listed in Table 4. **a** M_{PGV} versus M_{W-GCMT} *left panel* and m_b vs M_{PGV} *right panel*, respectively. **b** M_{W-SIL} versus M_{W-GCMT} *left panel* and m_b vs M_{W-SIL} *right panel*, respectively. The *black lines* in the figure are 1:1 lines showing how closely the values match. *Blue lines* the best fit obtained using GOR, whereas *green lines* the model proposed by WASON et al. (2012)

where $N(\geq M)$ is the number of earthquakes with magnitude at least as large as M. Consequently, M_C can be identified from data as the minimum magnitude at which the cumulative frequency magnitude distribution departs from the exponential decay (e.g. ZUNIGA and WYSS 1995). In this study, we used the maximum curvature method (WIEMER and WYSS

2000) to estimate M_C, and we estimated the *b value* using maximum likelihood (UTSU 1965). Figure 9a shows the results before and after the quality check of the catalogue. There are no strong differences in M_C, *b value* and *a* values using the two considered catalogues, but the linear part of the GR relation appears to fit the corrected catalogue better (right

Table 4

List of earthquakes plotted in Fig. 8

Dd/mm/yyyy	Hh:mm:ss	M_L	M_{W-SIL}	M_{W-GCMT}	M_{PGV}	M_b (ISC)
27/12/1992	12:23:20	4.2	3.7	–	4.7	4.3
20/08/1994	16:40:22	3.9	3.6	–	4.4	4.2
30/04/1995	00:57:57	3.7	3.5	–	4.1	3.9
14/10/1996	20:59:58	3.8	3.8	–	4.2	4.1
23/02/1997	00:35:47	3.6	3.6	–	4.0	3.7
23/02/1997	08:45:02	3.6	3.5	–	4.0	3.8
12/04/1997	23:04:44	3.8	3.8	–	4.2	3.9
24/08/1997	03:04:22	4.4	4.1	–	5.0	4.7
03/06/1998	06:47:42	3.6	3.8	–	4.0	–
04/06/1998	19:04:46	4.0	3.8	–	4.5	4.2
04/06/1998	21:36:54	4.7	4.4	5.4	5.3	5.1
04/06/1998	22:59:58	4.0	3.9	–	4.5	4.2
13/11/1998	10:38:34	4.6	4.5	5.1	5.2	4.7
14/11/1998	14:24:07	4.4	4.1	–	5.0	4.7
25/05/1999	13:19:40	4.0	3.7	–	4.5	4.1
27/09/1999	16:01:14	4.2	4.0	–	4.7	4.1
17/06/2000	15:40:41	5.5	6.2	6.5	6.3	5.7
17/06/2000	15:42:51	5.0	5.3	–	5.7	5.6
17/06/2000	15:45:27	4.6	4.8	–	5.2	5.3
17/06/2000	17:09:26	3.9	4.1	–	4.4	3.9
17/06/2000	17:40:17	4.4	4.1	5.0	5.0	4.6
21/06/2000	00:51:47	5.4	6.6	6.4	6.2	6.0
23/08/2003	02:00:11	4.3	4.4	5.1	4.9	4.7
06/03/2006	14:31:55	4.2	4.1	–	4.7	4.2
27/02/2007	05:24:23	3.9	3.6	4.9	4.4	–
27/02/2007	05:51:51	4.0	3.6	5.0	4.4	–
29/05/2008	15:46:00	5.3	5.1	6.3	6.1	5.8
29/05/2008	17:07:31	4.1	3.7	–	4.6	3.6
29/05/2008	17:09:42	3.8	3.4	–	4.2	3.5
29/05/2009	21:33:51	4.2	4.1	4.8	4.7	4.7
30/05/2009	13:35:21	4.0	3.3	–	4.5	4.3
19/06/2009	18:13:20	3.8	2.8	–	4.2	4.2
19/06/2009	20:37:13	3.8	2.9	–	4.2	4.0
25/06/2009	17:20:17	3.7	3.1	–	4.1	4.0
23/10/2010	20:34:31	4.2	3.1	4.9	4.7	–
23/10/2010	21:59:00	4.7	3.5	5.2	5.3	–
27/02/2011	09:06:00	3.6	3.0	–	4.0	3.5
27/02/2011	09:49:04	3.1	3.2	–	3.4	3.5
27/02/2011	17:27:37	3.8	3.3	–	4.2	3.7
03/01/2012	21:12:42	3.8	3.0	–	4.2	3.5
30/08/2012	11:59:04	3.9	4.0	–	4.4	4.1
09/05/2013	19:20:40	3.7	3.3	4.8	4.2	–
13/10/2013	07:34:06	4.7	4.5	5.2	5.3	–

panel in Fig. 9a). For the investigated area we estimate M_C as 0.79 ± 0.05, which demonstrates the SIL system's ability to reliably detect small earthquakes; the estimated *b value* is 0.85 ± 0.03.

In case of an aftershock sequence or changes to the seismic network, one would expect to see changes in M_C and *b value*. To investigate this, we checked for temporal variations in M_C and *b value* using the maximum curvature technique, a window size of 500 events, a moving window of 50 events, and a 25 % smoothing function (Fig. 9b).

The results show that both the M_C and the *b value* are affected by large earthquake sequences, such as the June 2000 and May 2008 sequences, which both included $M_W > 6.0$ events. The mainshock and the subsequent moderate magnitude earthquakes

Table 5

M_L central value, bin amplitude, mean values of M_W and two standard deviations (σ)

M_L bin	Mean M_W	2σ
−0.1–0.1	0.79	0.37
0.1–0.3	0.92	0.40
0.3–0.5	1.06	0.43
0.5–0.7	1.19	0.42
0.7–0.9	1.31	0.40
0.9–1.1	1.44	0.39
1.1–1.3	1.56	0.39
1.3–1.7	1.70	0.42
1.5–1.7	1.85	0.44
1.7–1.9	2.02	0.46
1.9–2.1	2.17	0.53
2.1–2.3	2.37	0.64
2.3–2.5	2.41	0.72

($M_W > 4.0$) in the following days, indeed, introduce the largest variation in M_C when it reaches values of about 1.4–1.5 (Fig. 9b, upper panel). In the case of *b value*, strange variations could be seen as for instance starting from 2000 until 2005 for the occurrence of a long aftershocks sequence following the 17 and 21 June 2000 earthquakes (Fig. 9b, lower panel). In particular, in this case the *b value* increased steadily reaching 1.4 after those events. We also note that the *b value* exceeds in many periods the value estimated from the GR relationship of all events during the considered time period (Fig. 9b). These results could be related to the behaviour of the GR curve (Fig. 9a). The GR curve has a high slope in the magnitude range 0.79–2.6, whereas the slope is low at magnitudes greater than 2.6. A possible explanation could be an interaction between tectonic and volcanic activity, which in Iceland are tightly linked. A similar result was obtained in Guagua Pichincha volcano (Ecuador) by LEGRAND *et al.* (2004). The authors suggested that a non-linear Frequency Magnitude Distribution (FMD) of GR may be understood as the superposition of various processes, such as classic elastic rupture (*b value* $\approx$ 1.00) and hydraulic fracturing (*b value* up to 2.0). Therefore, deviations from linearity in the FMD may be related to temporal and spatial variations in *b value* as observed in our results.

The spatial variations of the M_C and *b values* for South Iceland were achieved using the common catalogue-based mapping approach of WYSS *et al.* (1999) and WIEMER and WYSS (2000). The method consists of computing M_C and *b value* through FMD, using a combination of a fixed number of events, N in each node of a spatial grid and the constant radius method, which consists of selecting all earthquakes within a certain distance. This means that if a node in the grid does not meet the requirement of *N* earthquakes, then those events within distance *R* from the node are included, to fulfil the requirement. In particular, we used a spatial grid of 0.03° in latitude and 0.07 in longitude and $R = 15$ km. The fixed number of earthquakes, *N* to compute the GR was 300 and the minimum number of earthquakes required to estimate M_C was 30. Finally the maps were smoothed by using a Gaussian kernel filter with sigma equal to 3.

In Fig. 10a we show the results for the original catalogue; these results seem to be strongly influenced by the explosions near Reykjavík and Reykjanesbaer with very high *b values* and M_C (>2.0). The *b value* for the revised catalogue is in the range 0.8–1.0 except for the eastern zone, which is characterized by high *b value*, probably due to a small number of earthquakes (Fig. 10b). The central area of the South Iceland Seismic Zone is characterized by low values of M_C ($\approx$ 0.6–0.8) whereas the eastern and western areas show higher values (>1.0). In particular, the detection capability of the seismic network decreases near the Reykjanes peninsula coast, probably due to the proximity to the city, and in the eastern SISZ where the seismic network configuration is more spread out.

5.2. Seismic Rate Analysis

In Fig. 11a, we plot the number of earthquakes as a function of time to explore possible changes in seismicity rate, considering only the earthquakes with magnitude greater than M_C (0.79). The trend of the revised catalogue is not markedly different from the original catalogue, although of course the cumulative number of earthquakes is different. Three prominent steps in the curve's slope are identified corresponding to the April 1994, June 2000, and May 2008 earthquake sequences in the investigated area (dashed line in Fig. 11a). There is a change in slope (i.e.
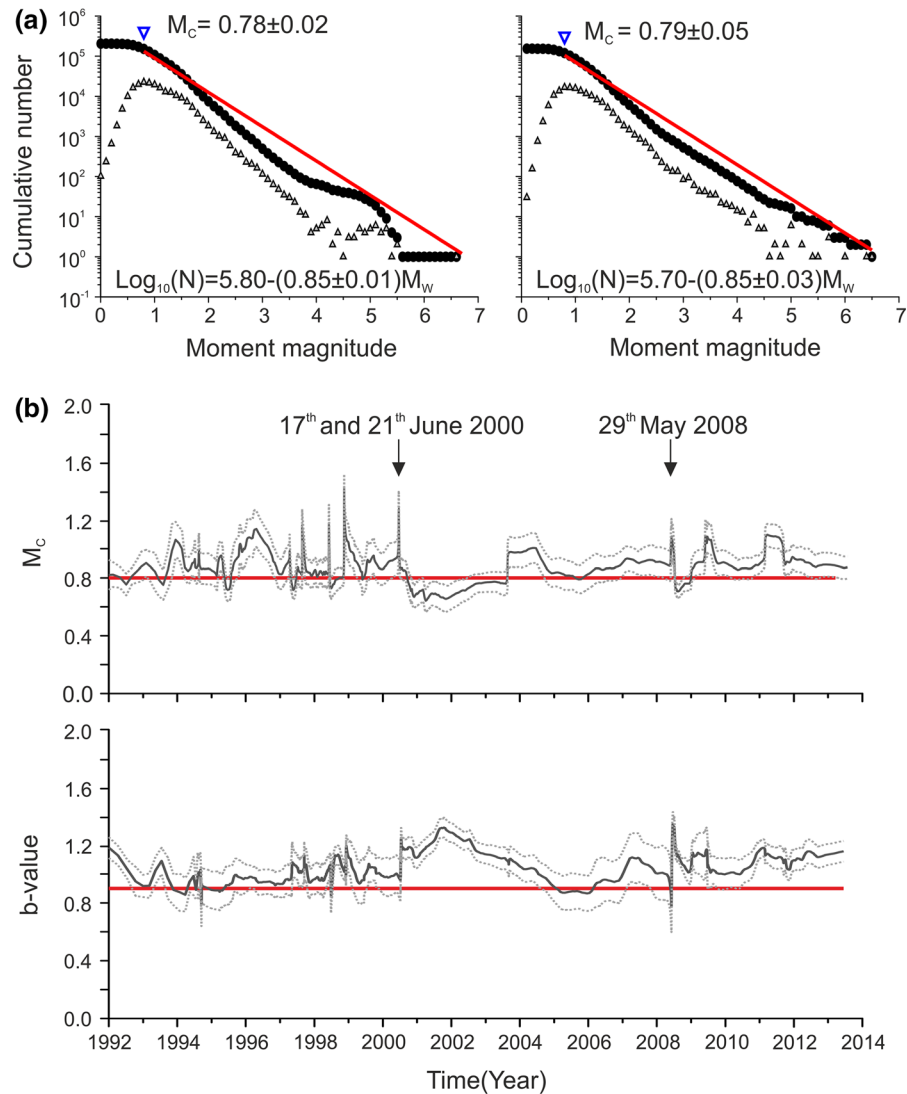
Figure 9

a Magnitude distribution of the original catalogue (*left panel*) and of the revised catalogue (*right panel*). **b** M_C (*top panel*) and *b* value (*lower panel*) as a function of time. *Red line* the M_C and *b* value estimated from the GR relationship of all events during the considered time period and the *black arrows* the onset of the June 2000 and May 2008 earthquake sequences

increased average seismicity rate) between mid-1994 and 1999, which is due to an intense volcano-tectonic interaction episode in the Hengill region (FEIGL *et al.* 2000). The effect on the overall trend, caused by the Hengill swarm, is evident by removing all the seismicity around this region (black curve in Fig. 11a) and verifying that the slope becomes fairly regular for the studied period (1991–2013). It is also interesting to observe that the seismicity filter demonstrates more clearly another step in the

cumulative curve in addition to those related to the occurrence of strong earthquakes (June 2000 and May 2008). In particular, the step linked to the two earthquakes of November 1998, previously hidden in the Hengill swarm, appears evident (Fig. 11a).

There is also a noticeable change around 2011. This change in rate may be explained by the fact that the seismic network was improved in the eastern part of the investigated area in late 2010. Distribution of earthquakes in the studied area was also investigated
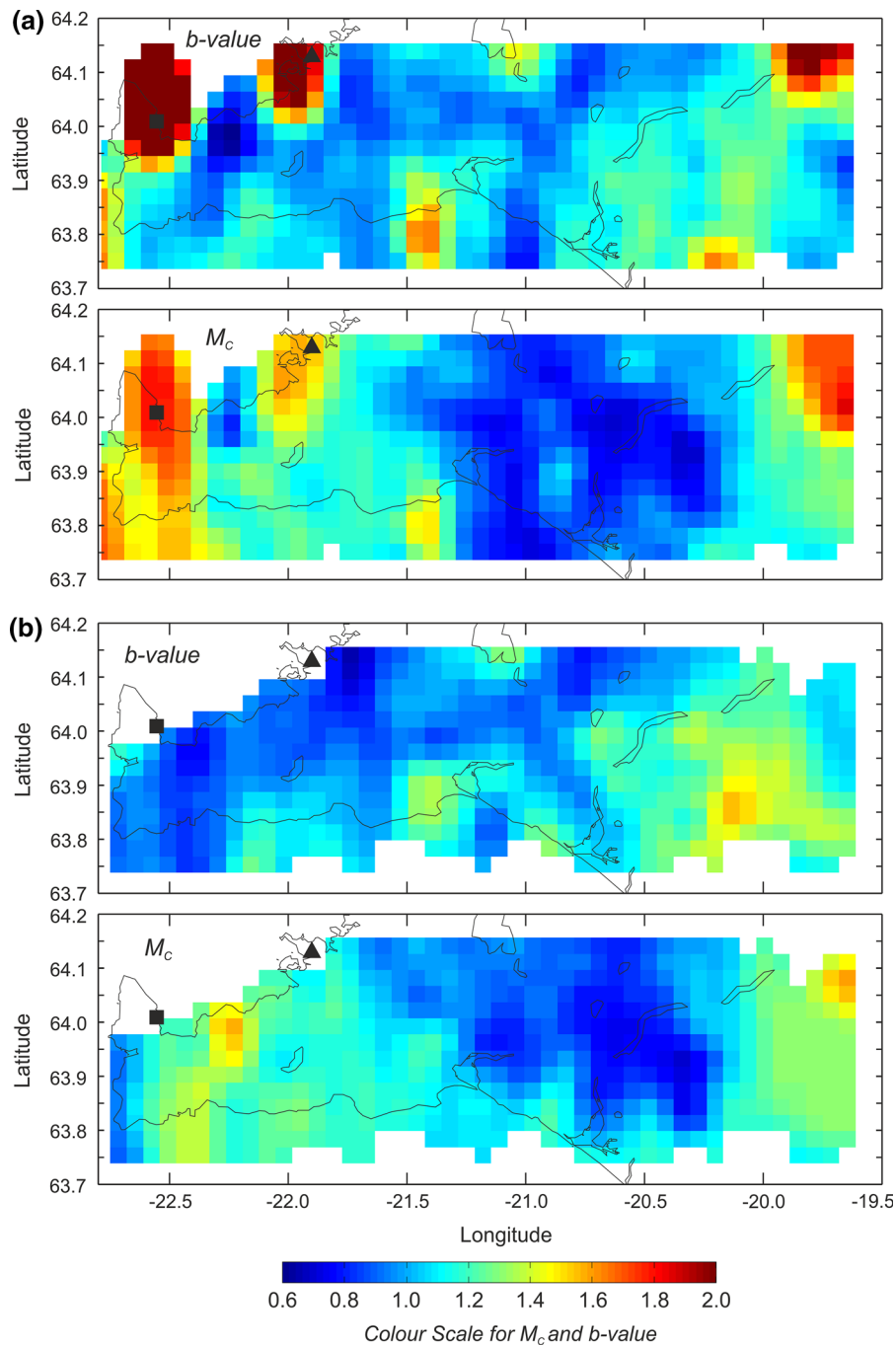
Figure 10

b value and M_C maps for the **a** the original catalogue and **b** revised catalogue. *Black triangle* and *rectangle* the position of Reykjavík and Reykjanesbaer, respectively

by drawing an earthquake density map (Fig. 11b), as the logarithm of earthquakes per square km, obtained using a spatial grid of 0.03° in latitude and 0.07 in longitude. From this map we can identify the zones with major occurrence of earthquakes. The seismicity is not uniformly distributed, but rather it is
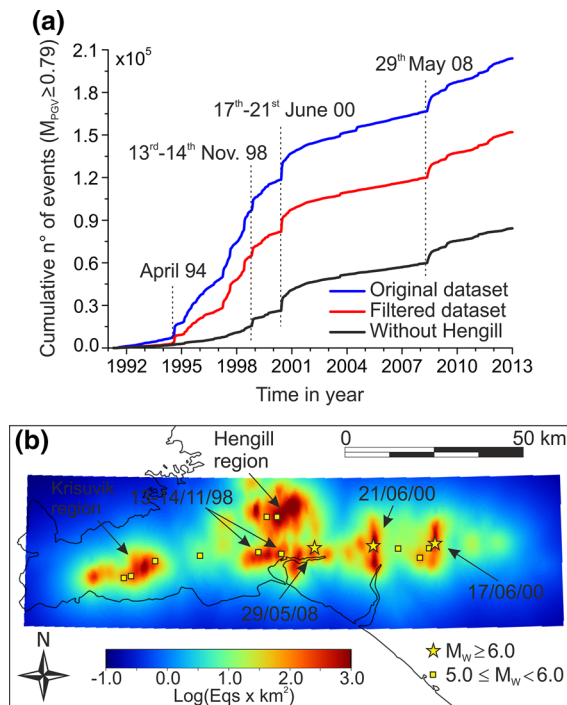
Figure 11

a Number of earthquakes versus time before and after revising the catalogue. **b** Earthquake density in which *stars* indicate the areas with high earthquake activities

concentrated around the major active faults, geothermal centres in the Krísuvík region and the geothermal/volcanic centre in Hengill (Fig. 11b).

6. Concluding Remarks

Twenty years after the installation of the SIL system, we have analysed the South Iceland earthquake catalogue to understand its strengths and weaknesses. In a sense, this is necessary preliminary work for any future study on seismicity forecasting or regional seismic hazard assessment. The revised catalogue is available upon request to the authors.

The main results of this study can be summarized as follows:

- We explored the consequences of using the network criteria method to filter the SIL catalogue in Iceland. In this region, where the emphasis is on recording microseismicity, but the network is not as dense as in many other parts of the world, we found the filter to be too strict: almost all microearthquakes were filtered out because they did not have enough arrival time picks. As an alternative, we suggest a filter based on the multivariate distribution of hypocentral uncertainties. This filter, based on Mahalanobis distance, results in a catalogue with smaller uncertainties and more events than the network criteria method (75 % of events pass the filter).

- We searched the catalogue for quarry blasts that were incorrectly identified as earthquakes. We found and removed 502 such events (~ 0.4 % of earthquakes in the filtered catalogue).

- We noted and corrected several problems with the local magnitude and so-called local moment magnitude estimates reported in the SIL catalogue. In particular, the magnitude of the largest events is often underestimated, and the magnitude of smaller events following large events was often overestimated.

- We compared estimates of the magnitude of completeness, b value, and seismicity rate based on the original catalogue and the filtered, corrected catalogue and identified possible explanations for the differences.

This work emphasizes the importance of carefully assessing an earthquake catalogue before proceeding with further analysis, and as such we hope that our revised catalogue will be used for future studies and models of seismicity in South Iceland.

REFERENCES

AMBRASEYS, N.N., and SIGBJÖRNSSON, R. (2000), *Re-Appraisal of the Seismicity of Iceland*, Polytechnica-Engineering Seismology, No. 3, Earthquake Engineering Research Centre, University of Iceland.

ANGELIER, J., SLUNGA, R.F., BERGERAT, F., STEFANSSON, R., and HOMBERG, C. (2004), *Perturbation of stress and oceanic rift extension across transform faults shown by earthquake focal mechanisms in Iceland*, E.P.S.L., *219*, 271–284.

ANTONIOLI, A., BELARDINELLI, M. E., BIZZARI, A., and VOGFJÖRD K. S. (2006). *Evidences of instantaneous triggering during the seismic sequence of year 2000 in south Iceland.* J. Geophys. Res., *111*. doi:10.1029/2005JB003935.

ÁRNADÓTTIR, T.H., GEIRSSON, H., and EINARSSON P. (2004). *Co-seismic stress changes and crustal deformation on the Reykjanes Peninsula due to triggered earthquakes on June 17, 2000.* J. Geophys. Res., *109*, B09307. doi:10.1029/2004JB003130.

BERGERAT, F., and ANGELIER, J. (2000), *The South Iceland Seismic Zone: tectonic and seismotectonic analyses revealing the evolution from rifting to transform motion*, Journal of Geodynamics, *29*, 211–231.

BÖDVARSSON, R., RÖGNVALDSSON, S.T., JAKOBSDÓTTIR, S.S., SLUNGA, R., and STEFÁNSSON, R., (1996), *The SIL data acquisition and monitoring system*, Seism. Res. Lett., *67*, 35–46.

BÖDVARSSON, R., RÖGNVALDSSON, S.T., SLUNGA, R., and KJAR-TANSSON, E. (1999), *The SIL data acquisition system-at present an beyond year 2000*, Phys. Earth Planet. Inter., *113*, 89–101.

BONDAR, I., MYERS, S.C., ENGDAHL, E.R., and BERGMAN, E.A. (2004), *Epicentre accuracy based on seismic network criteria*, Geophys. J. Int., *156*, 483–496.

CASTELLARO, S., MULARGIA, F., and KAGAN, Y.Y. (2006), *Regression problems for magnitudes*, Geophys. J. Int., *165*, 913–930. doi:10.1111/j.1365-246X.2006.02955.x.

CLIFTON, A. E., PAGLI, C., JÓNSDÓTTIR, J. F., EYTHÓRSDÓTTIR, K., and VOGFJÖRD, K. (2003). *Surface effects of triggered fault slip on Reykjanes Peninsula, SW Iceland.* Tectonophysics, *369*, 145–154.

CLIFTON, A., and EINARSSON P. (2005). *Styles of surface rupture accompanying the June 17 and 21, 2000 earthquakes in the South Iceland Seismic Zone.* Tectonophysics, *396*, 141–159.

CLIFTON, A.E., and KATTENHORN, S.A. (2006), *Structural architecture of a highly oblique divergent plate boundary segment*, Tectonophysics, *419*, 27–40.

DECRIEM, J., ÁRNADÓTTIR, T., HOOPER, A., GEIRSSON, H., SIGMUNDSSON, F., KEIDING, M., ÓFEIGSSON, B.G., HREINSDÓTTIR, S., EINARSSON, P., LAFEMINA, P., and BENNETT, R.A. (2010). *The 2008 May 29 earthquake doublet in SW Iceland*, Geophys. J. Int. (2010) *181*, 1128–1146. doi: 10.1111/j.1365-246X.2010.04565.x.

DZIEWONSKI, A.M., CHOU, T.A., and WOODHOUSE, J.H. (1981), *Determination of earthquake source parameters from waveform data for studies of global and regional seismicity*, J. Geophys. Res., *86*, 2825–2852. doi:10.1029/JB086iB04p02825.

EINARSSON, P. (1991), *Earthquakes and present-day tectonism in Iceland*, Tectonophysics, *189*, 261–279.

EINARSSON, P. (2008), *Plate boundaries, rifts and transforms in Iceland*, JÖKULL, *58*, 35–58.

EINARSSON, P., BJÖRNSSON, S., FOULGER, G., STEFÁNSSON, R. AND SKAFTADÓTTIR, T. (1981) *Seismicity Pattern in the South Iceland Seismic Zone*, in Earthquake Prediction (eds D. W. Simpson and P. G. Richards), American Geophysical Union, Washington, D. C. Maurice Ewing Series *4*, 141–151, doi:10.1029/ME004p0141.

EKSTRÖM, G., NETTLES, M., and DZIEWONSKI, A.M. (2012), *The global CMT project 2004-2010: Centroid-moment tensors for 13,017 earthquakes*, Phys. Earth Planet. Inter., 200–201, 1–9. doi:10.1016/j.pepi.2012.04.002.

ESHAGHI, A., TIAMPO, K.F., GHOFRANI, H., and ATKINSON, G.M. (2013), *Using Borehole Records to Estimate Magnitude for Earthquake and Tsunami Early-Warning Systems*, Bull. Seismol. Soc. Am., *103*(4), 2216–2226. doi:10.1785/0120120319.

EVERITT, B.S. (2005), *An R and S-PLUS companion to multivariate analysis*, Springer: London, p. 221.

FEIGL, K.L., GASPERI, J., SIGMUNDSSON, F., and RIGO, A. (2000). *Crustal deformation near Hengill volcano, Iceland 1993–1998: Coupling between magmatic activity and faulting inferred from elastic modelling of satellite radar interferograms.* J. Geophys. Res., *105* (B11), 25655–25670.

GOMBERG, J.S., SHEDLOCK, K.M., and ROECKER, S.W. (1990), *The effect of S-Wave arrival times on the accuracy of hypocenter estimation*, Bull. Seism. Soc. Am., *80*, 1605–1628.

GUDMUNDSSON, G.B., VOGFJÖRD, K.S. and THORBJARNARDÓTTIR, B.S. (2006). *SIL data status report*, in: *PREPARED – third periodic report, February 1, 2005 – July 31, 2005*. R. STEFÁNSSON et al. (Eds.). Icelandic Meteorological Office report, no 06008, VI-ES-05, Appendix 3, pp 127–131.

GULIA, L., WIEMER, S., and WYSS, M. (2012), *Catalog artifacts and quality controls*, Community Online Resource for Statistical Seismicity Analysis. doi:10.5078/corssa-93722864. http://www.corssa.org.

GUTENBERG, R., and RICHTER, C.F. (1944), *Frequency of earthquakes in California*, Bulletin of the Seismological Society of America, *34*, 185–188.

HABERMANN, R.E. (1987), *Man-made changes of seismicity rates*, Bull. Seism. Soc. Am., *77* (1), 141–159.

HACKMAN, M.C., KING, G.C.P., and BILHAM, R. (1990), *The mechanics of the South Iceland Seismic Zone*, Journal of Geophysical Research. doi:10.1029/90JB01043.

HJALTADÓTTIR, S. (2009) *Use of relatively located microearthquakes to map fault patterns and estimate the thickness of the brittle crust in Southwest Iceland. Sub-surface fault mapping in Southwest Iceland*, Master's thesis, Faculty of Earth Sciences, University of Iceland, pp. 104. ISBN 978-9979-9914-6-5. http://hdl.handle.net/1946/3990.

HJALTADÓTTIR, S., VOGFJORD, K. S., AND SLUNGA, R. (2005), *Mapping subsurface faults in southwest iceland using relatively located microearthquakes*, Geophysical research abstracts, *7*, 06664.

HUSEN, S., and HARDEBECK, J.L. (2010), *Earthquake location accuracy*, Community Online Resource for Statistical Seismicity Analysis. doi:10.5078/corssa-55815573. http://www.corssa.org.

JAKOBSSON, S.P., HONSSON, J., and SHIDO, F. (1978), *Petrology of the western Reykjanes Peninsula, Iceland*, Journal of Petrology, *19*, 669–705.

KEIDING, M., ÁRNADÓTTIR, TH., STURKELL, E., GEIRSSON, H., and LUND, B. (2008). *Strain accumulation along an oblique plate boundary: The Reykjanes Peninsula, southwest Iceland.* Geophys. J. Int., *172*(1):861–872. doi:10.1111/j.1365-246X.2007.03655.x.

LEGRAND, D., VILLAGÓMEZ, D., YEPES, H., and CALAHORRANO, A. (2004) *Multifractal dimension and b value analysis of the 1998–1999 Quito swarm related to Guagua Pichincha volcano activity,*

Ecuador, J. Geophys. Res., *109*, B01307. doi:10.1029/2003 jb002572.

LIN, T., and WU, Y.M. (2010), *Magnitude determination using strong ground motion attenuation in earthquake early warning*, Geophys. Res. Lett., *7*, L07304. doi:10.1029/2010GL042502.

MADIGAN, D., BARTLETT, P., BÜHLMANN, P., CARROLL, R., MURPHY, S., ROBERTS, G., SCOTT, M., TÁVARE, S., TRIGGS, C., WANG, J-L., WASSERSTEIN, R., and ZUMA, K. (2014), *Statistics and science: a report of the London Workshop on the Future of the Statistical Sciences.* http://bit.ly/londonreport. last accessed 31 July 2014.

MIGNAN, A., WOESSNER, J. (2012), *Estimating the magnitude of completeness for earthquake catalogs*, Community Online Resource for Statistical Seismicity Analysis. doi:10.5078/corssa-00180805. http://www.corssa.org.

PÉTURSSON, G.G. and VOGFJÖRD, K.S. (2009), *Attenuation relations for near- and far field peak ground motion (PGV, PGA)and new magnitude estimates for large earthquakes in SW-Iceland*, Icelandic Meteorological Report no VI 2009-012, pp 43. ISSN 1670-8261.

ROTH, F. (2004), *Stress Changes Modelled for the Sequence of Strong Earthquakes in the South Iceland Seismic Zone Since 1706*. Pure & Applied Geophysics, *161*, 1305–1327.

RÖGNVALDSSON, S.T. and SLUNGA, R. (1993), Routine fault plane solutions for local networks: A test with synthetic data, Bull. Seismol. Soc. Am., *83*(4), 1232–1247.

SCHORLEMMER, D., and WOESSNER, J. (2008), *Probability of detecting an earthquake*, Bull. Seismol. Soc. Am., *98*(5), 2103–2117. doi:10.1785/0120070105.

SLUNGA, R., NORRMAN, P., and GLANS, A. (1984), *Seismicity of Southern Sweden – Stockholm: Försvarets Forskningsanstalt*, FOA Report, C2 C20543-T1, 106 pp.

STEFÁNSSON, R., BÖÐVARSSON, R., SLUNGA, R., EINARSSON, P., JAKOBSDÓTTIR, S.S., BUNGUM, H., GREGERSEN, S., HAVSKOV, J., HJELME, J., and KORHONEN, H. (1993), *Earthquake prediction research in the South Iceland seismic zone and the SIL project*, Bull. Seism. Soc. Am., *83*, 696–716.

STORCHAK, D.A., DI GIACOMO, D., BONDÁR, I., ENGDAHL, E.R., HARRIS, J., LEE, W.H.K., VILLASEÑOR, A., and BORMANN, P.

(2013). *Public Release of the ISC-GEM Global Instrumental Earthquake Catalogue (1900–2009)*, Seism. Res. Lett., *84*(5), 810–815. doi:10.1785/0220130034.

TORMANN, T., WIEMER, S., HAUKSSON, E. (2010). *Changes in reporting Rates in the Southern California Earthquake Catalog, Introduced by a New Definition of Ml*, Bull. Seism. Soc. Am., *100*(4), 1733–1742.

UTSU, T. (1965), *A method for determining the b-value in a formula logN = a−bm showing magnitude frequency relation for earthquakes*, Hokkaido Univ. Geophys. Bull., *13*, 99–103, in Japanese with English abstract.

VOGFJÖRD, K.S., KJARTANSSON, E., SLUNGA, R., HALLDÓRSSON, P., HJALTADÓTTIR, S., GUDMUNDSSON, G.B., SVEONBJÖRNSSON, H., ÁRMANNSDÓTTIR, S., THORBJARNARDÓTTIR B., and JAKOBSDÓTTIR, S. (2012). *Development and implementation of seismic early warning processes in South-west Iceland*, Icelandic Meteorological Report n° VI 2010-012, pp 83. ISSN 1670-8261.

WASON, H.R., DAS, R., and SHARMA M.L. (2012), *Magnitude conversion problem using general orthogonal regression*, Geophys. J. Int., *190*(2), 1091–1096.

WIEMER, S., and BAER, M. (2000), *Mapping and removing quarry blast events from seismicity catalogs*, Bull. Seism. Soc. Am., *90*, 525–530.

WIEMER, S., and WYSS, M. (2000), *Minimum magnitude of completeness in earthquake catalogs: examples from Alaska, the Western United States, and Japan*, Bull. Seism. Soc. Am., *90*, 859–869.

WOESSNER, J., and WIEMER, S. (2005), *Assessing the quality of earthquake catalogues: Estimating the magnitude of completeness and its uncertainty*, Bull. Seismol. Soc. Am., *95*. doi:10.1785/012040007.

WYSS, M., HASEGAWA, A., WIEMER, S. and UMINO, N. (1999), *Quantitative mapping of precursory seismic quiescence before the 1989, M 7.1, off-Sanriku earthquake, Japan*, Annali di Geophysica, *42*, 851–86.

ZUNIGA, F.R., and WYSS, M. (1995), *Inadvertent changes in magnitude reported in earthquake catalogs: their evaluation through b-value estimates*, Bull. Seism. Soc. Am., *85*, 1858–1866.